Fabrication of concave silicon micro-mirrors

Yueh Sheng Ow,* Mark B. H. Breese, and Sara Azimi

Physics Department, National University of Singapore, Lower Kent Ridge Road, 119260, Singapore
*g0601170@nus.edu.sg

Abstract: We have fabricated spherical and cylindrical concave micro-mirrors in silicon with dimensions from 20 µm to 100 µm. The fabrication process involves standard photolithography followed by large area ion beam irradiation and electrochemical anodisation in a HF electrolyte. After thermal oxidation the silicon surface roughness is less than 2 nm. We also present a multilayer porous silicon distributed Bragg reflector fabricated on concave silicon surfaces which selectively reflect and focus a band of wavelengths from a parallel beam of incident white light. Development of such low roughness concave microstructures opens up new applications in areas such as silicon photonics and quantum information science.

© 2010 Optical Society of America

OCIS codes: (130.0250) Optoelectronics; (230.1480) Bragg reflectors; (230.4000) Microstructure fabrication; (330.1690) Color; (160.6000) Semiconductor materials

---

References and links

1. F. Merenda, M. Grossenbacher, S. Jeney, L. Forró, and R. P. Salathé, "Three-dimensional force measurements in optical tweezers formed with high-NA micromirrors," Opt. Lett. **34**(7), 1063–1065 (2009).
2. F. Merenda, J. Rohner, J. M. Fournier, and R. P. Salathé, "Miniaturized high-NA focusing-mirror multiple optical tweezers," Opt. Express **15**(10), 6075–6086 (2007).
3. C. H. Lin, S. Y. Wen, and W. Y. Hsu, "Variable optical attenuator with tunable nonsmooth curved mirror," Jpn. J. Appl. Phys. **43**, 7764–7768 (2004).
4. Y. Aoki, Y. Shimada, and K. Iga, "Collimation characteristics of planar microlens for parallel optical interconnect," Opt. Rev. **7**(6), 483–485 (2000).
5. M. Trupke, E. A. Hinds, S. Eriksson, E. A. Curtis, Z. Moktadir, E. Kukharenka, and M. Kraft, "Microfabricated high-finesse optical cavity with open access and small volume," Appl. Phys. Lett. **87**(21), 211106 (2005).
6. G. Q. Cui, J. M. Hannigan, R. Loeckenhoff, F. M. Matinaga, M. G. Raymer, S. Bhongale, M. Holland, S. Mosor, S. Chatterjee, H. M. Gibbs, and G. Khitrova, "A hemispherical, high-solid-angle optical micro-cavity for cavity-QED studies," Opt. Express **14**(6), 2289–2299 (2006).
7. P. Horak, B. G. Klappauf, A. Haase, R. Folman, J. Schmiedmayer, P. Domokos, and E. A. Hinds, "Possibility of single-atom detection on a chip," Phys. Rev. A **67**(4), 043806 (2003).
8. S. E. Morin, C. C. Yu, and T. W. Mossberg, "Strong Atom-Cavity Coupling Over Large Volumes and the Observation of Subnatural Intracavity Atomic Linewidths," Phys. Rev. Lett. **73**(11), 1489–1492 (1994).
9. T. Pellizzari, S. A. Gardiner, J. I. Cirac, and P. Zoller, "Decoherence, Continuous Observation, and Quantum Computing: A Cavity QED Model," Phys. Rev. Lett. **75**(21), 3788–3791 (1995).
10. F. M. Matinaga, A. Karlsson, S. Machida, Y. Yamamoto, T. Suzuki, Y. Kadota, and M. Ikeda, "Low-threshold operation of hemispherical microcavity single-quantum-well lasers at 4-K," Appl. Phys. Lett. **62**(5), 443–445 (1993).
11. D. C. Appleyard, and M. J. Lang, "Active particle control through silicon using conventional optical trapping techniques," Lab Chip **7**(12), 1837–1840 (2007).
12. J. Albero, L. Nieradko, C. Gorecki, H. Ottevaere, V. Gomez, H. Thienpont, J. Pietarinen, B. Päivänranta, and N. Passilly, "Fabrication of spherical microlenses by a combination of isotropic wet etching of silicon and molding techniques," Opt. Express **17**(8), 6283–6292 (2009).
13. T. E. Bell, P. T. J. Gennissen, D. DeMunter, and M. Kuhl, "Porous silicon as a sacrificial material," J. Micromech. Microeng. **6**(4), 361–369 (1996).
14. M. Navarro, J. M. LopezVillegas, J. Samitier, J. R. Morante, J. Bausells, and A. Merlos, "Electrochemical etching of porous silicon sacrificial layers for micromachining applications," in 7th Workshop on Micromachining, Micromechanics and Microsystems in Europe (MME 96, 1996), pp. 131–132.
15. E. J. Teo, M. B. H. Breese, E. P. Tavernier, A. A. Bettiol, F. Watt, M. H. Liu, and D. J. Blackwood, "Three-dimensional microfabrication in bulk silicon using high-energy protons," Appl. Phys. Lett. **84**(16), 3202–3204 (2004).
16. E. J. Teo, M. B. H. Breese, A. A. Bettiol, D. Mangaiyarkarasi, F. Champeaux, F. Watt, and D. J. Blackwood, "Multicolour Photoluminescence from Porous Silicon using Focused High-energy Helium Ions," Adv. Mater. **18**(1), 51–55 (2006).
17. M. B. H. Breese, F. J. T. Champeaux, E. J. Teo, A. A. Bettiol, and D. J. Blackwood, "Hole transport through proton-irradiated p-type silicon wafers during electrochemical anodization," Phys. Rev. B **73**(3), 035428 (2006).

18. D. Mangaiyarkarasi, O. Y. Sheng, M. B. H. Breese, V. L. S. Fuh, and E. T. Xioasong, "Fabrication of large-area patterned porous silicon distributed Bragg reflectors," Opt. Express **16**(17), 12757–12763 (2008).
19. Y. S. Ow, M. B. H. Breese, Y. R. Leng, S. Azimi, E. J. Teo, and X. W. Sun, "Micromachining of amplitude and phase modulated reflective computer generated hologram patterns in silicon," Nucl. Instrum. Methods Phys. Res. B **268**(9), 1416–1421 (2010).
20. V. Lehmann, Electrochemistry of Silicon: Instrumentation, Science, Materials and Applications (Wiley-VCH 2002).
21. G. Lérondel, R. Romestain, and S. Barret, "Roughness of the porous silicon dissolution interface," J. Appl. Phys. **81**(9), 6171–6178 (1997).
22. A. A. Busnaina, "An Experimental Study of Megasonic Cleaning of Silicon Wafers," J. Electrochem. Soc. **142**(8), 2812 (1995).
23. K. K. Lee, D. R. Lim, L. C. Kimerling, J. Shin, and F. Cerrina, "Fabrication of ultralow-loss Si/SiO(2) waveguides by roughness reduction," Opt. Lett. **26**(23), 1888–1890 (2001).
24. L. Lai, and E. A. Irene, "Limiting Si/SiO2 interface roughness resulting from thermal oxidation," J. Appl. Phys. **86**(3), 1729–1735 (1999).
25. H. Seidel, L. Csepregi, A. Heuberger, and H. Baumgartel, "Anisotropic etching of crystalline silicon in alkaline-solutions," J. Electrochem. Soc. **137**(11), 3612–3626 (1990).
26. X. J. Qiu, X. W. Tan, Z. Wang, G. Y. Liu, and Z. H. Xiong, "Tunable, narrow, and enhanced electroluminescent emission from porous-silicon-reflector-based organic microcavities," J. Appl. Phys. **100**(7), 074503 (2006).
27. D. Mangaiyarkarasi, M. B. H. Breese, and Y. S. Ow, "Fabrication of three dimensional porous silicon distributed Bragg reflectors," Appl. Phys. Lett. **93**(22), 221905 (2008).

1. Introduction

1.1 Concave mirrors and lenses

A concave surface profile in the micron regime is of interest because of its ability to focus incoming light into a spot. In bio-sensing or cell trapping devices, incoming laser that is focused by such a concave mirror acts like optical tweezers to trap/push particles with the optical gradient/scattering force [1,2]. In the field of micro-electro-mechanical-systems (MEMS) and optoelectronics, it may be used as a variable optical attenuator [3] or to produce an enhanced and localized light signal for parallel low loss optical interconnect systems [4]. From these concave profiles, it is possible to further fabricate concave optical cavities by coupling two such mirrors together or with an optical fiber [5]. These kind of concave cavities are of interest in quantum information science, particularly in the fabrication of atom chips [5,6] or for small particle detection [7]. Single photons may be produced on demand using atoms in such a concave cavity to have entanglement effects with a shared cavity photon [8,9].

There have been several techniques reported to fabricate concave mirrors on different materials. These include diffusion of ion dopants on glass [4], melting photoresist disks to obtain a spherical shape followed by dry etching on GaAs [10] and trapping of air bubbles in borosilicate glass [6]. Fabricating concave mirrors on silicon is especially important to allow for easy integration into the well-developed Si microelectronics infrastructure, as well as for good reproducibility and up-scaling purposes. Functional optical trapping techniques on Si surfaces are also very important [11]. The fabrication of concave mirrors in Si is not trivial, nevertheless, it was reported by Trupke in Ref [5] where concave profiles were created by isotropic wet etching of Si through circular apertures in a lithographic mask using a mixture of HF and HNO_3 under continuous agitation. This was primarily motivated by applications in quantum information sciences, particularly for the studies of cavity quantum electrodynamics (CQED). A similar method to fabricate concave profiles on Si is reported in Ref [12]. The use of thermal oxide (SiO_2) and low-stress silicon nitride (Si_3N_4) as a hard mask together with isotropic wet etching of Si in an etch solution containing etch solution consists of HF and HNO_3 was used to create concave profiles on Si which were used subsequently as molds to form microlenses on polymers.

1.2 Silicon machining via ion beam irradiation with sacrificial porous silicon

Porous silicon (PSi) has been used traditionally as a sacrificial material for various techniques of micro-machining Si [13,14]. More recently, Si micromachining has been performed using high-energy ion beam irradiation [15,16]. In this approach, MeV ions, typically protons or

helium ions are used to irradiate wafers which results in a localized increase in resistivity for p-type Si wafers by creating point defects along the ion trajectories [17]. Irradiation is usually performed by focusing ions to spot sizes of a few hundred nanometers in a nuclear microprobe and used to directly irradiate patterns on the wafers. In a more recent development, a facility was built for wafer irradiation using a uniform, large area ion beam which was defocused by the lens system of a nuclear microprobe [18,19]. Irradiation is achieved by a thick, patterned photoresist on the wafer surface acting as a mask to shield the underlying Si from irradiation. The work reported here uses this large area method of irradiation. Increased resistivity in irradiated Si locally reduces the current flow during subsequent electrochemical anodization [17], hence the PSi formation slows down with increased fluence. If the fluence is high enough, the hole current flow may be completely stopped and the formation of PSi ceases completely in the irradiated regions. The underlying Si microstructure may then be revealed by removing the PSi with potassium hydroxide (KOH).

Given the range of applications for controllably fabricated concave, micrometer-scale mirrors and microcavities, here we discuss a new process for making such structures in Si using a process of ion irradiation and electrochemical anodization. This process has been used to fabricate spherical concave profiles which produce a point focus. In addition, concave cylindrical profiles which produce line focus have also been fabricated. This same process may be used to fabricate any elliptical profile between these geometries as well.
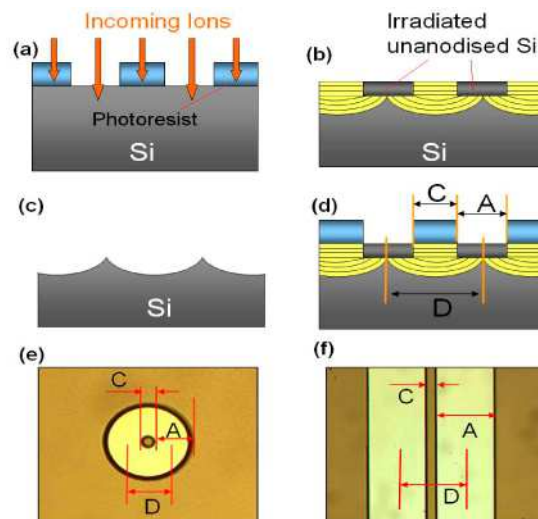
2. Experimental

Fig. 1. (a), (b) and (c) shows the cross sectional schematic process flow for the fabrication of the concave mirrors and concave cylinders. (d) defines the parameters A, C and D as the width of the irradiated annulus/lines, diameter of the central aperture and the final diameter of the mirror/cylinder respectively. (e) and (f) show the photoresists patterns used for fabricating the concave mirrors and cylinders respectively and the equivalent parameters A, C and D of the cylinders and mirrors in planer view.

A schematic of the fabrication process to produce spherical concave surfaces is shown in Fig. 1a-c. Annuli were patterned (Fig. 1e) using standard ultraviolet lithography on a 7μm thick AZ 4620 photoresist spin coated on to 0.02 Ω.cm p-type wafers (Fig. 1a). The exposed annuli were then irradiated with a large area beam of 600 keV helium ions, which have a range of ~2.3 μm in silicon. The helium ions are completely stopped in areas covered with photoresist and create defects only in the exposed annuli. The wafers were irradiated with a fluence of 3×10^{14} ions/cm^2, high enough to stop PSi from forming at the exposed surfaces. Ion irradiation is thus used here to turn the irradiated annuli into a HF resistant mask, with PSi

only forming at the surface within the small central aperture. A curved etch front naturally forms after the top irradiated region is undercut (Fig. 1b), since PSi formation is isotropic for 0.02 Ω.cm p-type wafers [20]. Moreover, such highly doped wafers typically have a low surface roughness of a few nanometers after the removal of PSi [21].

From Fig. 1d, the diameter, D, of each concave mirror is determined by the diameter, C, of the central aperture plus twice the half-width, A/2, of the annulus. The diameter of the concave surface does not increase further once the two PSi etch fronts meet halfway underneath each irradiated annulus. The same process is used for the fabrication of concave cylindrical structures with the same parameters A, C and D as in Fig. 1 and the cylindrical structures have the same cross sectional profiles. The only difference is that instead of irradiating annular patterns, lines are irradiated instead (Fig. 1f). Concave mirrors and cylinders with two different diameters, D = 20μm and D = 100μm, were fabricated here.

After irradiation, the photoresist was removed with Nano Strip[TM] (Cyantek Inc) and the wafer electrochemically etched at 70mA/cm^2 for different periods depending on the dimensions of the annuli. For example, a concave mirror/cylinder with a diameter of D = 100μm, has a central aperture diameter of C = 18μm and the width of the annulus is A = 82μm. The anodized depth has to be at least half of A, equal to ~41μm in this example, so that the irradiated annulus is completely undercut. At the end of the anodisation, a large electropolishing current pulse of ~800mA/cm^2 was applied to detach the thick PSi and the irradiated Si annuli from the underlying concave Si surface.

3. Results and discussions

3.1 Spherical and cylindrical micro-mirrors

Large arrays of cylindrical concave lines and spherical concave mirrors may be fabricated simultaneously using the above mentioned process, as shown in Fig. 2. One of the features of this fabrication technique is that the location of each mirror or cylinder may be precisely controlled, unlike the random mirror fabrication by trapping bubbles in borosilicate [6]. The diameters may be very well controlled as well since it does not increase further once the two etch fronts meet under the irradiated Si annulus. The accuracy in determining both the location and diameters of these mirrors is limited primary by the patterning of the photoresist during the UV lithography step. The fabricated arrays of concave profiles may very well be use as molds or templates to produce microlenses in polymers [12]. Figure 2a shows an optical image of one such concave cylindrical structure where the microscope stage was positioned so as to capture the focal length of the cylinder where incoming light was focused into a single bright line in the center of the cylinder. Figure 2b shows a cleaved cross section of a similar structure with D = 100μm where the concave cylindrical cross-section can be seen.

In Fig. 3a, concave cylinders with D = 20μm were formed by creating multilayer PSi with alternating porosity and cleaved to show their cross sections. In this case, formation of a multilayer serves the purpose of tracking the progression of the PSi formation through the central apertures. PSi layers formed from the central apertures are initially parallel to the surface, however, once the formation goes past the end of range of the helium ion irradiation, curve profiles begins to form, as in Fig. 1b. It can be seen that the etch fronts are parallel and the diameter of each cylindrical etch front increases until the point when the two fronts of PSi formation meet underneath the irradiated regions.
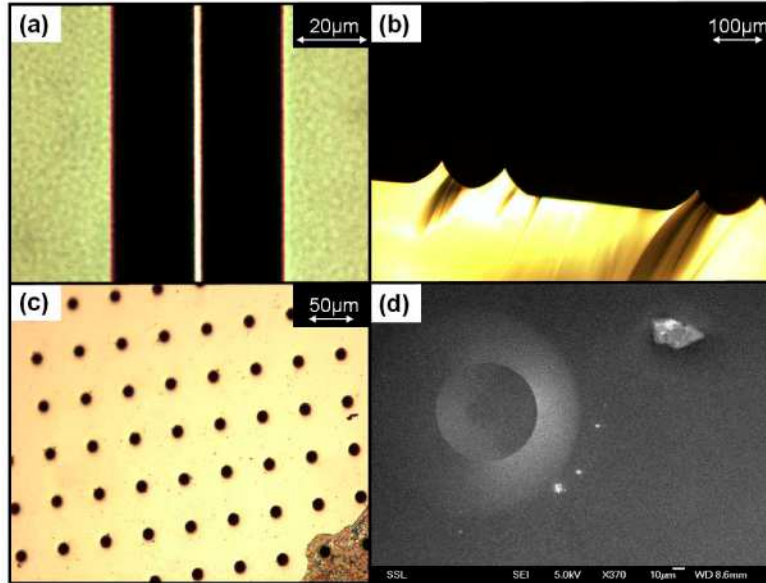
Fig. 2. (a) and (b) shows concave cylindrical mirrors. (c) and (d) show concave spherical mirrors. (a) is an optical image of a D = 20 μm concave cylinder. (b) shows a cross section of a concave cylinder with D = 100 μm, which may also represent the cross sections of D = 100 μm concave mirrors. (c) is an optical image of a large array of D = 20 μm concave mirrors. (d) is an SEM image of a single D = 100 μm concave mirror.
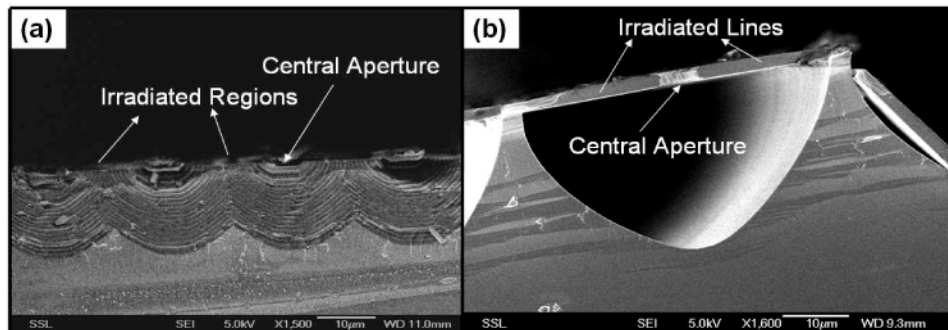

Fig. 3. (a) is a SEM cross section image of a concave cylinder with D = 20 μm fabricated with a PSi multilayer above the concave silicon surface. (b) shows a SEM cross section of a concave cylinder anodized such that the irradiated regions are not fully undercut and the PSi removed with diluted KOH.

In Fig. 3b, two long lines 30μm in width and 5μm apart were irradiated. They were then anodized and the anodization stopped just before the two etch front meet each other. PSi was then removed by immersing the sample in a diluted KOH solution. The sample was then cleaved and its cross section imaged with an SEM. As the irradiated regions were not fully undercut, they remain after the removal of PSi, demonstrating the ability to produce a mask resistant to electrochemical anodisation in HF directly on the Si surface itself. This way of producing a resistant mask prior to etching is fairly straightforward compared to the many steps required to create hard masks as reported in Ref [5,12].

3.2 Characterization

After PSi removal, samples were cleaned using a megasonic cleaner [22] to remove any remaining surface debris. The surface roughness was then further reduced on three different

samples by iterative thermal oxidation in air. AFM (atomic force microscope) measurements were carried out after every few hours of oxidation and removal of the oxide in a diluted (2%) HF solution [23]. The r.m.s. (root-mean-square) roughness versus oxidation time is shown in Fig. 4a. In the best case, the mirror roughness was reduced from 3.4nm to 1.7nm, while in the two other samples the roughness was reduced to about 2.5nm. This is consistent with the work by Lai [24] who reported that the final roughness achievable from this method is determined by its initial roughness.
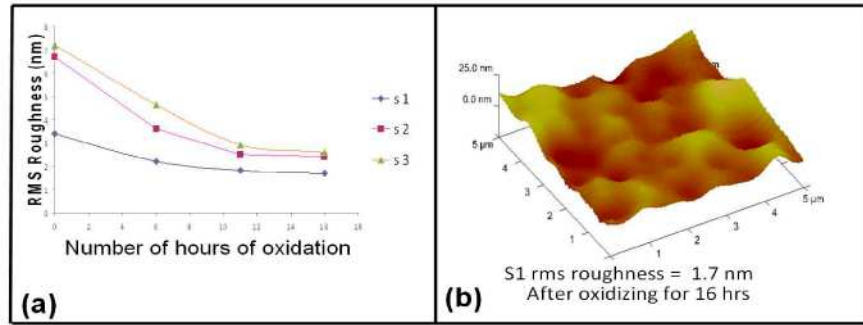

Fig. 4. (a) is a plot showing the r.m.s. roughness versus oxidization time for three different samples s1, s2 and s3. (b) shows the AFM image of the sample with the lowest r.m.s. roughness of 1.7 nm over an area of 5 x 5μm.

Electropolishing instead of KOH was used to remove the PSi because KOH is an anisotropic etchant in which the etch rate is plane dependent. For a concave mirror, the effect of any KOH exposure is immediately apparent since such a wide angular range of crystalline planes are exposed, as shown in Fig. 5a. Such "blossom" patterns resulting from KOH etching was reported previously [25], and rapidly ruins the uniform profile of any concave surface. In comparison, the PSi on the concave mirror in Fig. 5c which was removed by electropolishing has no 'blossom' patterns and the concave mirror is able to focus incoming light into a single bright spot.
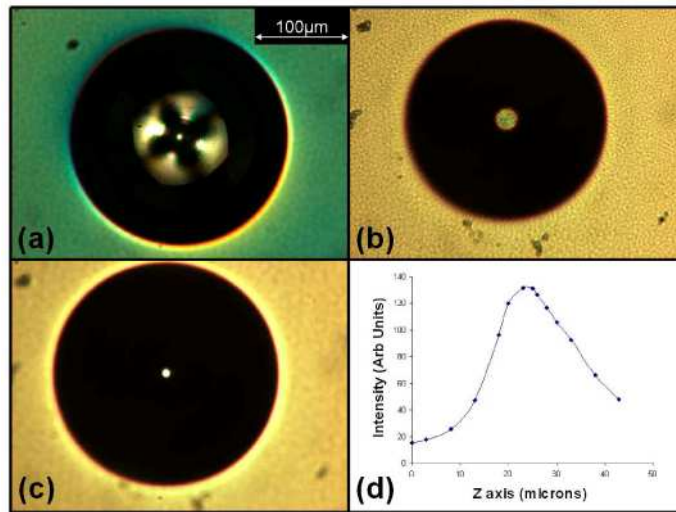

Fig. 5. (a) shows the 'blossom' pattern on a concave mirror resulting from the anisotropic KOH removal of PSi. In (b), the Psi was removed by electropolishing. (c) is an optical image of a concave mirror where the bottom of mirror is in focus. (d) is a plot of the intensity of the bright spot in the center of a concave mirror versus the microscope stage vertical position measured from the bottom of the concave mirror. The highest intensity is measured to be ~25 μm from the bottom of the mirror and this may be taken to be the focal length of the mirror.

In Fig. 5b, c and d, the focal length of a D = 100μm concave mirror was characterized using an optical microscope. In Fig. 5b, the microscope was positioned with the base of the mirror in focus. The sample was then moved vertically downwards until the curved region of the mirror focuses into a bright spot in Fig. 5c. Intensity measurements of the spot are shown in Fig. 5d. The focal length is taken to be where the intensity of the central spot is the highest, equal to ~25μm here. This further shows that the concave mirrors are spherical since spherical mirrors have a focal length of half their radius.

3.2 Concave PSi multilayer distributed Bragg reflectors

Distributed Bragg reflectors are multilayer structures with alternating high and low refractive indices. Each layer has an optical thickness of $\lambda /4 = nd$, where n is the refractive index, d is the thickness and λ is the reflected wavelength. Through the multiple reflections from each successive layer, together with constructive and destructive interferences, a Bragg reflector is able to reflect at particular wavelength λ from an incident light orthogonal to the surface.

PSi was demonstrated to be a good material for the fabrication of such multilayered structures [26]. The refractive index n of a single PSi layer is dependent on the porosity which is in turn dependent on the current density used during the anodisation process. The formation of PSi is self-limiting, hence, to create a PSi based Bragg reflector, one just alternates the etch current densities during anodisation to create layers with alternating high/low refractive indices as in Fig. 3a. The use of ion irradiation to slow down PSi formation was successfully used to tune the reflectivity of such Bragg reflectors [18] as well as to fabricate three dimensional Bragg reflectors [27]. Here we describe the fabrication of PSi multilayer Bragg reflectors on the concave etched surfaces, giving the ability to selectively reflect and focus particular wavelengths.
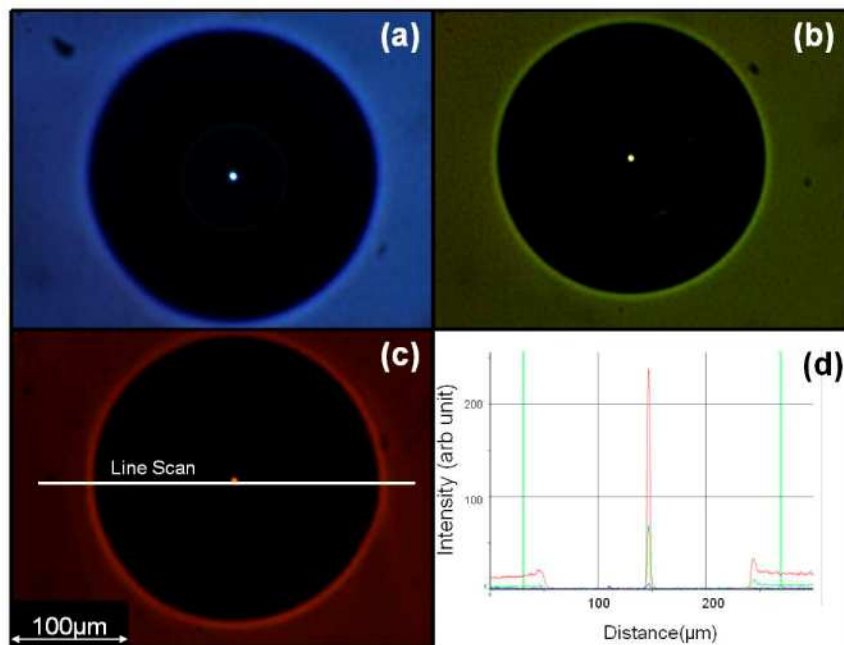

Fig. 6. (a), (b) and (c) are optical images of concave Distributed Bragg mirrors designed to focused and reflect blue, green and red respectively. These concave Bragg mirrors are illuminated with white light and they correctly select and focused their respective colors. A line scan was taken across the red concave Bragg mirror as shown in (c) and is plotted in (d). The plot correctly show that red is the dominant color focused to a point.

The concave mirrors described above were then used to form concave multilayer PSi Bragg reflectors. Three samples were etched to select and focus red, green and blue at 630nm,

530nm and 450nm respectively from a white incident light. They were fabricated to have 20 sets of bilayers with alternating current densities of 10mA/cm^2 and 70mA/cm^2. The anodization thickness of each layer was varied to have different optical thickness *nd* corresponding to one quarter of their respective wavelength.

Figure 6a, b and c shows the optical images of successfully fabricated concave PSi Bragg reflectors designed to reflect blue, green and red. These concave Bragg reflectors were illuminated with a parallel white light source and the concave Bragg reflectors then select the respective wavelengths and focus them into a single spot. The reflectivity of the red-reflecting concave Bragg reflectors is further characterized in Fig. 6d. With the aid of a microscope, a line scan measuring the intensity of the red, green and blue spectral components was measured across the focused point (Fig. 6c) and plotted in Fig. 6d. The line scan shows the dominant red color that this mirror was designed to reflect and focus. It also shows that the mirror focuses the incoming light down to a beam spot of approximately 1µm (FWHM from Fig. 6d). This line scan plot very appropriately shows both the focusing and wavelength selective properties of these curved PSi Bragg reflectors concurrently. This work also demonstrates the ability to form curved PSi distributed Bragg reflectors, in which each layer remains parallel to those above and below it. While these Bragg Reflectors have been demonstrated for visible wavelengths, it can easily be extended to the infra-red simply by increasing the thickness of each layer in the multilayer.

4. Conclusion

We have fabricated Si concave spherical mirrors and concave cylinders with low roughness and demonstrated the ability to do so repeatedly and controllably. The location, diameters and the height of the concave mirrors and concave cylinders may be controlled and are limited primarily by the patterning of the photoresist patterns during the UV lithography step. These concave structures have a variety of applications ranging from MEMS and optoelectronics to lab-on-chip devices. They may also be used as templates or molds to produce microlenses on polymers. By using these concave mirrors in conjunction with plane mirrors, small optical cavities can be built for single atom detection or quantum information control through cavity QED effects. In addition, using these concave mirrors as a starting material, we have also fabricated concave PSi based Bragg reflectors which are able to have wavelength selective focus. This will be useful for telecommunications or to be used as optical interconnects.

Acknowledgements